J. Plasma Physics (2015), *vol.* 81, 305810107 © Cambridge University Press 2014
doi:10.1017/S0022377814000877

Collisional relaxation: Landau versus Dougherty operator

Oreste Pezzi†, F. Valentini and P. Veltri

Dipartimento di Fisica and CNISM, Università della Calabria, 87036 Rende (CS), Italy

(Received 18 June 2014; revised 28 August 2014; accepted 17 September 2014;
first published online 13 October 2014)

A detailed comparison between the Landau and the Dougherty collision operators has been performed by means of Eulerian simulations, in the case of relaxation toward equilibrium of a spatially homogeneous field-free plasma in three-dimensional velocity space. Even though the form of the two collisional operators is evidently different, we found that the collisional evolution of the relevant moments of the particle distribution function (temperature and entropy) are similar in the two cases, once an 'ad hoc' time rescaling procedure has been performed. The Dougherty operator is a nonlinear differential operator of the Fokker-Planck type and requires a significantly lighter computational effort with respect to the complete Landau integral; this makes self-consistent simulations of plasmas in presence of collisions affordable, even in the multi-dimensional phase space geometry.

1. Introduction

The longstanding problem of collisions in plasmas is a very fascinating and huge topic in the field of plasma physics and it has always been the subject of a relevant scientific effort. Many authors approached the study of collisional effects in plasmas (Landau 1936; Spitzer 1956; Lenard and Bernstein 1958), by modeling particle interactions through different operators with different physical features and mathematical structures.

The 'natural' operator that describes the Coulombian interactions between charged particles (in absence of wave-particle resonance) is the Landau integral operator (Landau 1936). The Landau collision integral is a nonlinear, integro-differential and Fokker-Planck type operator which satisfies the H-theorem for the entropy growth (Hinton and Hazeltine 1976). Due to its nonlinear nature and multi-dimensionality, any analytical and numerical approaches to the solution of the Landau integral results extremely complicated.

When studying plasma dynamics, collisions are usually considered either negligible (Vlasov model) or dominant such to maintain the distribution function Maxwellian (fluid model). For physical systems, such as the solar wind, that exhibit a weak, almost negligible collisionality, the kinetic and collisional approach is necessary, especially when physical processes of particle heating and consequent entropy growing are considered. In fact, on the basis of the H-theorem, collisions are the unique physical 'ingredient' that can thermalize free-energy and produce heating in general thermodynamic sense.

† Email address for correspondence: oreste.pezzi@fis.unical.it

https://doi.org/10.1017/S0022377814000877 Published online by Cambridge University Press

From the numerical point of view, a self-consistent collisional approach requires, in principle, simulation of the Landau equation for the particle distribution function coupled to the Maxwell equations for fields. Since the Landau operator is multi-dimensional, the computational cost to evaluate the Landau integral numerically is huge: for N gridpoints along each direction of the 3D-3V numerical phase space (3D in physical space and 3D in velocity space), the computation requires about N^9 operations at each time step. Remarkable attempts to attack the collisional problem numerically have been reported in Pareschi et al. (2000); Filbet and Pareschi (2002), where the authors proposed a spectral method for the numerical evaluation of the Landau collisional integral, based on the use of Fast Fourier Transform (FFT) routines. FFT routines allow to significantly reduce the computational weight with respect, for example, to the case of finite difference schemes, but also require to periodize the distribution function in the velocity domain as well as the Landau operator, thus introducing unphysical effects of fake binary collisions.

Due to the computational weight of the numerical approximation to the Landau integral, simplified collisional operators are usually considered to model collisionality. A major simplification consists in employing operators in differential form, which can be further reduced by decreasing their dimensionality in velocity space (Zakharov and Karpman 1963; O'Neil 1968). Of course, in reduced geometry velocity space, essential features of particle collisions are missed; nevertheless, reduced differential operators can be successfully employed to model collisionality in physical systems whose dynamical evolution is restricted to a preferential direction (Anderson and O'Neil 2007a,b). Recently, a detailed numerical study of these simplified operators (1D–1V) has been performed through Eulerian simulations (Pezzi et al. 2013, 2014a,b). In this study it has been shown that, among this class of operators, the most suitable operator to describe the effects of collisions in plasmas is the Dougherty one.

The general form of the Dougherty operator has been proposed by Dougherty (1964) to describe collisions among particles of the same species in 3D–3V physical systems. Moreover, this operator, even though it has been set up in a phenomenological way, satisfies the main properties of a good collisional operator (Anderson and O'Neil 2007a,b):

- it vanishes for any thermal equilibrium distribution function and it displays the Maxwellian distribution function as a long-time limit solution;
- it conserves particle number, momentum and energy;
- it describes the dominance of small-angle scattering through a velocity-space diffusion term.

However, since the Dougherty operator is explicitly phenomenological and it has not been formally derived from the Landau collisional operator, firstly it could give rise to evolution times which can be different from those predicted by the Landau operator by some numerical factor and secondly it does not describe the velocity dependence of the diffusion coefficients in velocity space.

For this reason, in the present paper we try to face the first problem by analyzing the behavior of the Dougherty operator (Dougherty 1964), as compared to that of the complete Landau integral, through a numerical investigation of the relaxation toward equilibrium of a spatially homogeneous plasma in absence of fields, in full three-dimensional geometry in velocity space. To perform this analysis, we describe numerically the return to equilibrium of several non-Maxwellian velocity distributions, and compare quantitatively the time evolution of the velocity distribution itself and of temperature and entropy. Interestingly enough, for the cases discussed in this work, the system evolution obtained when collisions are modeled through the Dougherty

https://doi.org/10.1017/S0022377814000877 Published online by Cambridge University Press

operator results very similar to the case where the full Landau integral is employed, provided an 'ad hoc' time rescaling is performed.

The structure of the paper is the following: in Sec. 2 the Landau and the Dougherty operators are explicitly described and compared from a theoretical point of view. Then, in Sec. 3, the effects of the two operators are compared through Eulerian simulations and the time rescaling factor which allows the Dougherty solution to closely approximate the Landau solution is discussed. Finally we summarize and conclude in Sec. 4, also discussing possible future developments.

2. Landau and Dougherty collisional operators

We consider here the collisional relaxation of a plasma in presence of collisions among particles of the same species (electron-electron or ion-ion). We assume that the plasma is spatially homogeneous and no field (self-consistent or external) is present.

The explicit form of the Landau operator, in dimensionless units, is the following:

$$\left.\frac{\partial f}{\partial t}\right|_{coll} = \frac{g \ln \Lambda}{8\pi} \frac{\partial}{\partial v_i} \int d^3v' \; U_{ij}(\mathbf{u}) \left[f(\boldsymbol{v}') \frac{\partial f(\boldsymbol{v})}{\partial v_j} - f(\boldsymbol{v}) \frac{\partial f(\boldsymbol{v}')}{\partial v'_j} \right], \tag{2.1}$$

$f(\boldsymbol{v})$ being the particle distribution function, normalized such as $\int d^3v \; f(\boldsymbol{v}) = n = 1$, $g = 1/n\lambda_D^3$ the plasma parameter, $\ln \Lambda \simeq -\ln g/3$ the Coulombian logarithm and $U_{ij}(\mathbf{u})$ the projector

$$U_{ij}(\mathbf{u}) = \frac{\delta_{ij} u^2 - u_i u_j}{u^3}, \tag{2.2}$$

where $\boldsymbol{u} = \boldsymbol{v} - \boldsymbol{v}'$ and $u = |\boldsymbol{u}|$. For brevity and clarity, we avoided to explicitly indicate the time dependence of the distribution function f. Moreover, the Einstein summation notation has been introduced.

The dimensionless Dougherty operator is the following:

$$\left.\frac{\partial f}{\partial t}\right|_{coll} = \frac{g \ln \Lambda}{8\pi} \frac{n}{T^{3/2}} \frac{\partial}{\partial v_j} \left[T \frac{\partial f(\boldsymbol{v})}{\partial v_j} + (v - V)_j \, f(\boldsymbol{v}) \right]. \tag{2.3}$$

where $n = \int d^3v f(\boldsymbol{v}) = 1$, $\mathbf{V} = 1/n \int d^3v \; \mathbf{v} f(\boldsymbol{v})$, $T = 1/3n \int d^3v (v - V)^2 f(\boldsymbol{v})$ respectively the density, the mean velocity and the temperature of the plasma.

In the previous equations, time is scaled to the inverse plasma frequency ω_p, lengths to the Debye length λ_D and velocities to the thermal speed v_{th}. From now on, all physical quantities will be scaled with these characteristic parameters.

It is worth to remark that both operators exhibit a similar Fokker-Planck structure, weighted with different coefficients, satisfy conservation of mass, energy and momentum and obeys an H-theorem (Dougherty 1964; Dougherty and Watson 1967; Hinton and Hazeltine 1976).

By looking at (2.1)–(2.3), one can realize that the projector $U_{ij}(\mathbf{u})$ that couples the velocity $\boldsymbol{v}$, at which the Landau collisional operator is evaluated, and the integration variable $\boldsymbol{v}'$ is absent in the Dougherty operator. This significantly simplifies the numerical solution, since the velocity integrals in the Dougherty operator (n, U and T) can be evaluated once for each time step in the simulation. In the case of spatially homogeneity, this reduces the computational cost from N^6 (Landau operator) to N^3 (Dougherty operator); for the general non-homogeneous case with three dimensions in physical space, the computational cost decreases from N^9 (Landau operator) to N^6 (Dougherty operator).

https://doi.org/10.1017/S0022377814000877 Published online by Cambridge University Press

3. Relaxation toward equilibrium: a numerical comparison

To begin this section, we shortly discuss the numerical strategy adopted to solve the collisional time evolution equation for the particle distribution function:

$$\frac{\partial f}{\partial t} = \left.\frac{\partial f}{\partial t}\right|_{coll}, \tag{3.1}$$

where $\partial f/\partial t|_{coll}$ is given by (2.1) for the case of the Landau operator and by (2.3) for the Dougherty operator. We will refer to (3.1) as the Landau or the Dougherty equation, depending on which collisional operator is used in the right-hand side.

The velocity derivatives in both Landau and Dougherty operator are evaluated numerically through a sixth-order centered finite difference scheme (Pezzi et al. 2013, 2014a), while for the time derivative a first-order Eulerian scheme has been employed. The explicit expressions of the schemes for the velocity derivatives are the following:

$$\left.\frac{\partial f}{\partial v_j}\right|_i = \frac{-f_{i-3} + 9f_{i-2} - 45f_{i-1} + 45f_{i+1} - 9f_{i+2} + f_{i+3}}{60\Delta v_j}, \tag{3.2}$$

$$\left.\frac{\partial^2 f}{\partial v_j^2}\right|_i = \frac{2f_{i-3} - 27f_{i-2} + 270f_{i-1} - 490f_i + 270f_{i+1} - 27f_{i+2} + 2f_{i+3}}{180\Delta v_j^2}; \tag{3.3}$$

i being a generic grid point along the velocity direction j and Δv_j the mesh size along the j-th velocity direction.

In the numerical velocity domain, f is set equal to zero for $|\boldsymbol{v}| > v_{\max}$, where $v_{\max} = 6v_{th,m}$ along each direction, where $v_{th,m} = \max\{v_{th,\parallel}, v_{th,\perp}\}$. The number of grid points used to discretize the velocity numerical domain has been chosen such that the ratio $\Delta v_j/v_{th,j}$ is almost constant for $j = x, y, z$. We typically use 101 grid points in v_z and 51 grid points in v_x and v_y.

The time step Δt is chosen in such a way to satisfy the Courant-Friedrichs-Levy condition for the numerical stability of time explicit finite difference schemes (Peyret and Taylor 1983).

In the following Sections, we will describe the comparison between Landau and Dougherty operators in different cases, i. e., initializing the computation with different initial particle velocity distributions. In Sec. 3.1 the evolution of a bi-Maxwellian velocity distribution is discussed. Then, in Sec. 3.2 we analyze the relaxation of velocity distributions with a plateau and a beam along one velocity direction. Finally, in Sec. 3.3, the evolution of a more 'distorted' velocity distribution, which comes out from a self-consistent 1D−1V Vlasov-Poisson simulation of nonlinear wave-particle interaction, is discussed.

3.1. *Bi-Maxwellian velocity distribution*

We consider the following bi-Maxwellian non-drifting velocity distribution:

$$f(v_x, v_y, v_z) = \frac{1}{(2\pi)^{3/2} T_\perp \sqrt{T_\parallel}} \exp\left[-\left(\frac{v_x^2}{2T_\perp} + \frac{v_y^2}{2T_\perp} + \frac{v_z^2}{2T_\parallel}\right)\right]. \tag{3.4}$$

Here, the subscript $\parallel$ indicates the z direction, while x and y are the perpendicular ($\perp$) directions. We define the temperature anisotropy as $A = T_\perp/T_\parallel$.

From the analytical point of view, by assuming that the distribution function remains a bi-Maxwellian during the process of collisional relaxation, one can integrate (3.1) in the case of both Landau and Dougherty operators to obtain the evolution equation for parallel and perpendicular temperatures.

https://doi.org/10.1017/S0022377814000877 Published online by Cambridge University Press

In the case of the Landau operator (Kogan 1961), one gets:

$$\frac{dT_\perp}{dt} = -\nu_L \left(T_\perp - T_\parallel\right), \tag{3.5}$$

$$\frac{dT_\parallel}{dt} = 2\nu_L \left(T_\perp - T_\parallel\right); \tag{3.6}$$

ν_T being a thermalization frequency given by:

$$\nu_L = \frac{g \ln \Lambda}{8\pi^{3/2} T_\parallel^{3/2}} \frac{-3 + \left(\tilde{A} + 3\right) \varphi(\tilde{A})}{\tilde{A}^2}, \tag{3.7}$$

where $\tilde{A} = A - 1$ and

$$\varphi(x) = \begin{cases} \tan^{-1}(\sqrt{x})/\sqrt{x} & x > 0 \\ 1 & x = 0 \\ \tanh^{-1}(\sqrt{-x})/\sqrt{-x} & x < 0 \end{cases} \tag{3.8}$$

It is worth noting that, in (3.5), (3.6), the total temperature $T = (2T_\perp + T_\parallel)/3$ remains constant in time.

In the same way, for the case of the Dougherty operator, one can easily get:

$$\frac{dT_\perp}{dt} = -\frac{2\nu_D}{3} \left(T_\perp - T_\parallel\right), \tag{3.9}$$

$$\frac{dT_\parallel}{dt} = 2\frac{2\nu_D}{3} \left(T_\perp - T_\parallel\right); \tag{3.10}$$

ν_D being a thermalization frequency written as:

$$\nu_D = \frac{g \ln \Lambda}{8\pi} \frac{n}{T^{3/2}}. \tag{3.11}$$

For the case of the Dougherty operator an evolution equation for the entropy $S = -\int d^3v f \ln f$ can be easily deduced, and reads:

$$\frac{dS}{dt} = n\nu_D \left[T \frac{T_\perp + 2T_\parallel}{T_\perp T_\parallel} - 3\right]. \tag{3.12}$$

Figure 1 shows the time evolution of parallel and perpendicular temperatures obtained from (3.5), (3.6) (black solid lines) and from (3.9), (3.10) (red dashed lines). In this specific case the initial anisotropy is $A = 4$, while the value of the plasma parameter is $g = 10^{-2}$. In this plot, time is normalized to the inverse Spitzer-Harm frequency (Spitzer 1956) ν_{SH}, that is the characteristic collisional frequency for relaxation processes in plasmas, and rescaled by a factor α. The value of α is set equal to 1 in the case of the Landau operator, while in the case of the Dougherty operator it is determined numerically in such a way to minimize the following function:

$$\sigma(\alpha) = \sqrt{\frac{1}{t_{\max}} \int_0^{t_{\max}} \left\{ \left[T_\parallel^{(L)}(t) - T_\parallel^{(D)}(\alpha t)\right]^2 + \left[T_\perp^{(L)}(t) - T_\perp^{(D)}(\alpha t)\right]^2 \right\} dt} \tag{3.13}$$

where $t_{\max}$ is the time at which the thermal equilibrium is established. This procedure gives $\alpha = 3.55$ for the Dougherty operator.

It is worth noting that rescaling the time by $\alpha = 3.55$ in the case of the Dougherty operator corresponds to rescaling the thermalization frequency ν_D by $1/\alpha$; in other words, the collisional effect of the Dougherty operator is made 'slower' than it would be originally.

https://doi.org/10.1017/S0022377814000877 Published online by Cambridge University Press

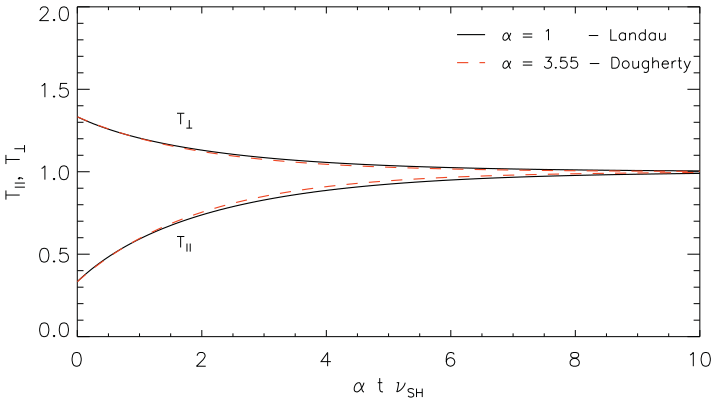


FIGURE 1. Time evolution of parallel and perpendicular temperatures obtained from (3.5), (3.6) (black solid lines) and (3.9), (3.10) (red dashed lines). The initial anisotropy is $A = 4$ and the plasma parameter $g = 10^{-2}$.

As it is clear from Fig. 1, when rescaling the time as explained above, the evolution of perpendicular and parallel temperatures obtained through the Landau equations (3.5), (3.6) and the Dougherty equations (3.9), (3.10) looks closely similar for many Spitzer-Harm times. We have checked that the value of the rescaling factor α does not depend on the value of g.

The analytical predictions for the time evolution of $T_\perp$ and $T_\parallel$ provide excellent benchmarks to check the direct numerical solution of equation (3.1). Therefore we solved numerically (3.1) in the case of the Landau operator and of the Dougherty operator, through the Eulerian algorithm shortly presented previously. Then, we compared the results of these simulations for the evolution of $T_\perp$ and $T_\parallel$ with the theoretical solutions. In these direct simulations the initial condition for the velocity distribution is given by (3.4) with $A = 4$ and the plasma parameter is $g = 10^{-2}$.

In Fig. 2(a) the evolution of $T_\perp$ and $T_\parallel$ is reported for the case in which the Landau operator is used in the right-hand side of (3.1). The analytical curves from (3.5), (3.6) are indicated as black solid lines, while the results of the direct simulation as red stars. In the same way, Fig. 2(b) shows the comparison between theory and numerical results for the case of the Dougherty operator. In both cases we get a very good agreement between analytical and numerical results. Again, the time scaling factor is $\alpha = 1, 3.55$ for the case of the Landau operator and of the Dougherty operator respectively.

Finally, in Fig. 2(c) we report the entropy growth obtained through the direct simulation of (3.1), in the case of the Landau operator (red stars), of the Dougherty operator (blue stars). The black solid line indicates the analytical solution from the time evolution of S from (3.12). Here, we point out that at time $t \simeq 1.5\nu_{SH}^{-1}$ the Landau solution slightly departs from the Dougherty solution even when time is rescaled by the factor $\alpha = 3.55$. A better agreement has been recovered for $\alpha = 3.35$. It is worth noting that, in both cases, the final temperature and the total entropy growth are in accord with the thermodynamical prediction on the final temperature and on the entropy variation between the initial condition (three Maxwellian distribution functions with different temperatures considered as isolated systems) and the equilibrium distribution functions at saturation (three Maxwellian distribution functions with the same temperature). This shows that the numerically

https://doi.org/10.1017/S0022377814000877 Published online by Cambridge University Press

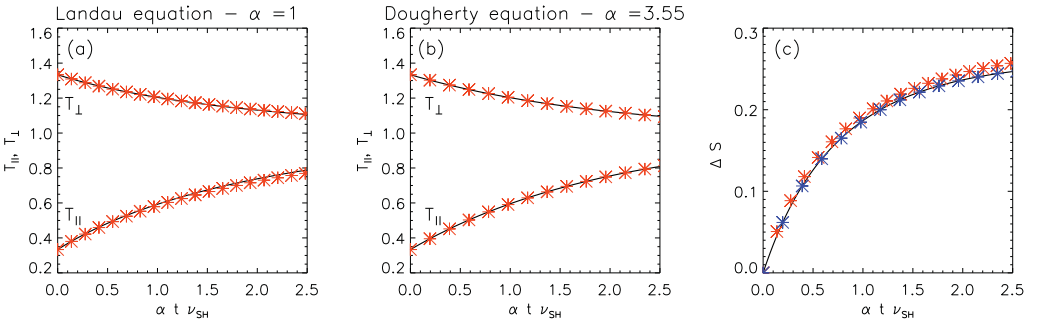


FIGURE 2. (a) Time evolution of the parallel and perpendicular temperatures for the Landau operator case. The black solid line represents the time evolution of the moments equations [(3.5), (3.6)], while the red dots correspond to the time evolution of the temperatures obtained from the numerical evolution of (3.1). (b) Time evolution of the parallel and perpendicular temperatures for the Dougherty operator case. The black solid line represents the time evolution of the moments equation [(3.9), (3.10)], while the red dots correspond to the time evolution of the temperatures obtained from the numerical evolution of (3.1). (c) Time evolution of the entropy growth obtained from (3.12) and from the numerical evolution of the (3.1) for the case of the Landau operator (red dots) and the Dougherty operator (blue dots), respectively.

produced entropy variation is negligible with respect to the entropy variation produced by the collisional terms.

Eulerian algorithms allow for a clean description (almost noise-free) of the velocity distribution. Figures 3(a)–(d) show four snapshots of the velocity distribution at four different times for a Dougherty simulation of equation (3.1) with initial anisotropy $A = 8$ and $g = 10^{-2}$. The sequence of plots illustrates how collisions work to restore the spherical shape of the velocity distribution, which corresponds to the isotropic Maxwellian configuration.

3.2. *Plateau and Beam velocity distributions*

In order to investigate whether the time rescaling procedure allows in general to reproduce the collisional Landau relaxation through the simplified Dougherty operator, in this Section we follow numerically the collisional evolution of velocity distributions with sharp gradients in one velocity direction. In particular, we considered a velocity distribution with a plateau along v_z (f_p) at $t = 0$ and a velocity distribution with a beam along v_z (f_b) at $t = 0$. This kind of velocity distributions are usually generated by resonant wave-particle interaction processes and are very common features recovered, for example, in solar-wind spacecraft observations (Marsch 2006) and in laboratory plasma experiments (Valentini et al. 2006; Driscoll et al. 2009).

For these new set of simulations the plasma parameter is $g = 10^{-2}$. The explicit expressions of the initial velocity distributions are:

$$f_p(v_z) = f_0(v_z) - \left[f_0(v_z) - f_0(v_p)\right] \cdot \left[1 + \left(\frac{v_z - v_p}{dv_p}\right)^{m_p}\right]^{-1} \tag{3.14}$$

$$f_b(v_z) = f_0(v_z) + \frac{n_b}{\sqrt{2\pi T_b}} \exp\left[-\frac{(v_z - V_b)^2}{2T_b}\right] \tag{3.15}$$

being $f_0(v_z) = 1/\sqrt{2\pi}\ \exp[-v_z^2/2]$, $v_p = 1.44$, $m_p = 8$, $dv_p = 0.5$ and $n_b = 0.17$, $V_b = 2.2$ and $T_b = 0.1$.

https://doi.org/10.1017/S0022377814000877 Published online by Cambridge University Press

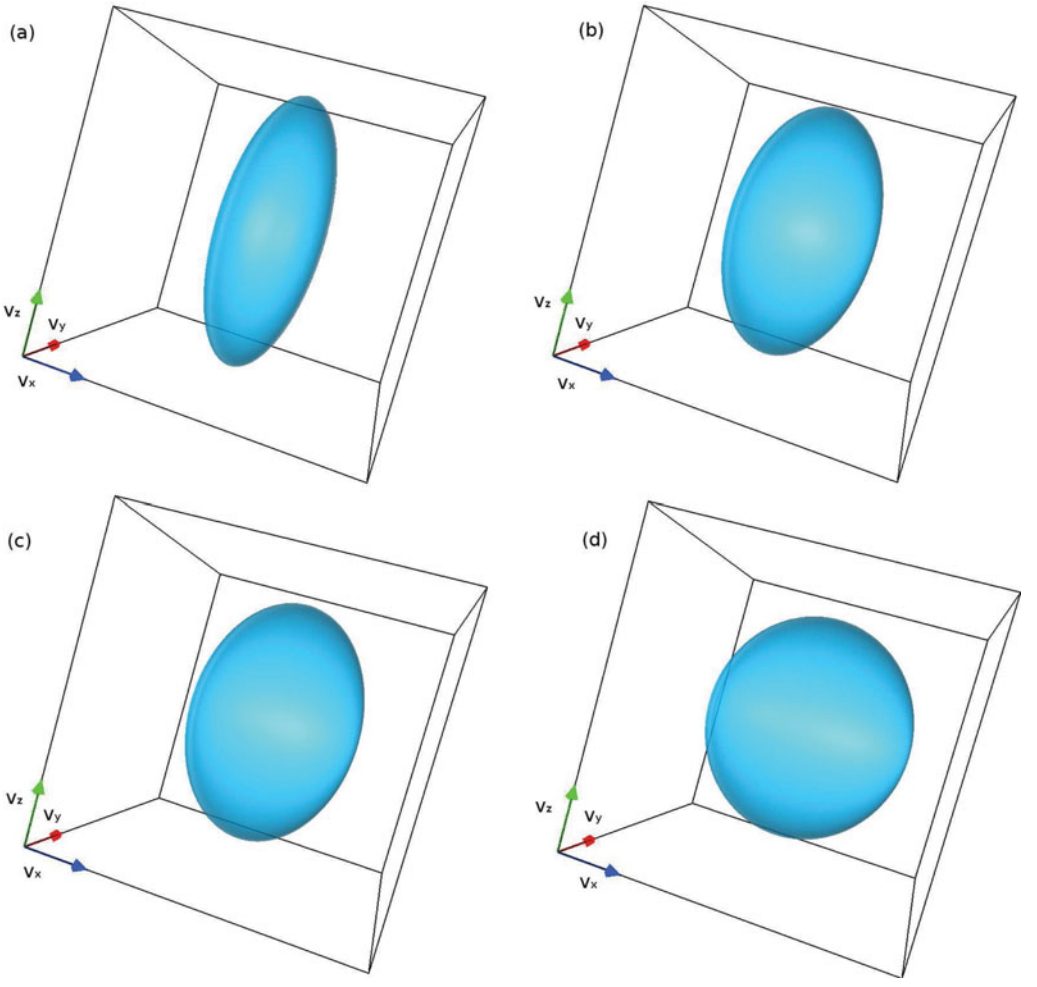


FIGURE 3. Snapshot (iso-contour levels) of the distribution function in the whole 3V space at four different times: $\alpha\ t_1\ \nu_{SH} = 0.00$ (a), $\alpha\ t_2\ \nu_{SH} = 0.70$ (b), $\alpha\ t_3\ \nu_{SH} = 1.38$ (c) and $\alpha\ t_4\ \nu_{SH} = 4.13$ (d).

Figures 4(a) and (b) show the initial velocity distributions f_p and f_b, respectively. Panels (c), (d) in the same figure display the time evolution of S obtained through the Landau operator (black solid line) and through the Dougherty operator (red stars), for the initial conditions f_p and f_b respectively. The rescaling factor is given the value $\alpha = 1, 3.55$ for the Landau operator and the Dougherty operator, respectively. We note that, for the plateau initial condition f_p, the Landau solution and the Dougherty solution almost superpose one on another, once time has been rescaled. A slight discrepancy is recovered for the case of the beam initial condition f_b.

A better agreement between Landau solution and Dougherty solution can be obtained slightly modifying the value of the scaling parameter α (better choices would be $\alpha = 3.35$ for the plateau initial condition and $\alpha = 3.75$ for the beam initial condition), which, however, remains very close to the value $\alpha = 3.55$ predicted from the analytical considerations in the previous section.

https://doi.org/10.1017/S0022377814000877 Published online by Cambridge University Press

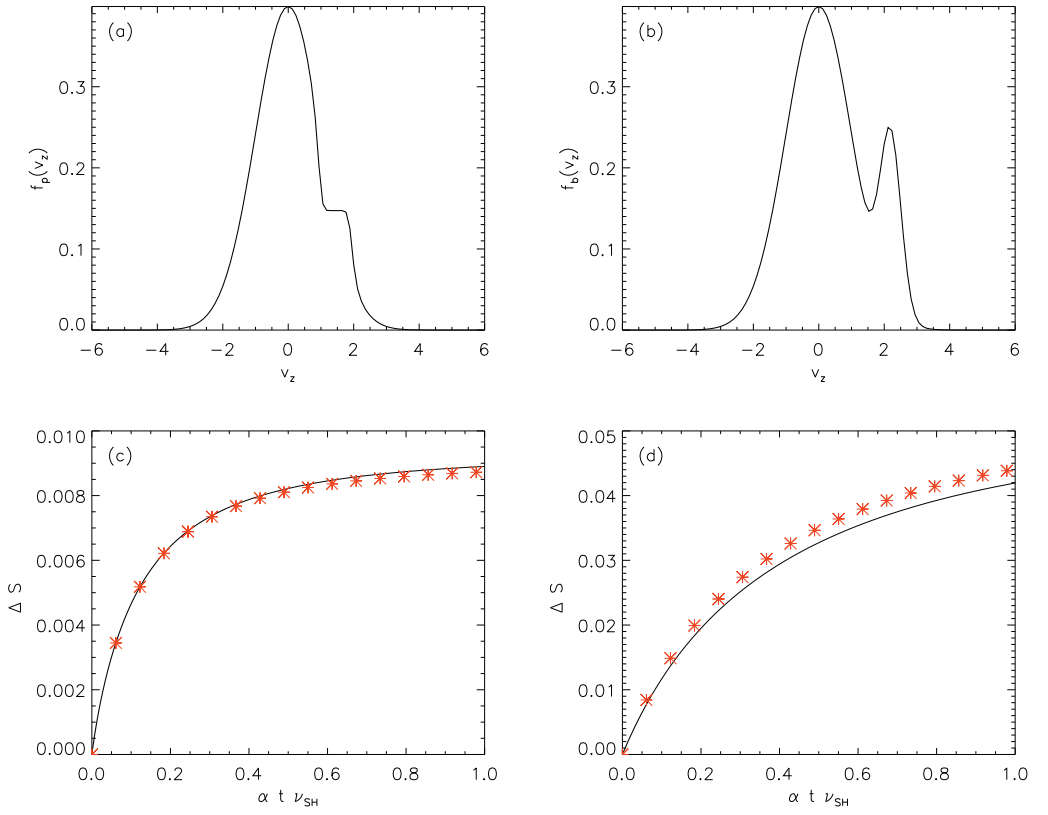


FIGURE 4. In the top row, the initial velocity distributions functions along v_z are shown for the plateau case [equation (3.14)] (a) and for the beam case [equation (3.15)] (b). In the bottom row, the entropy growth is presented for the Landau operator (black solid line) and for the Dougherty operator (red dashed line) for the plateau case (c) and for the beam case (d).

3.3. *Trapped particle distribution function*

As a final case, in this section we compare Landau and Dougherty operators in the process of collisional relaxation of a velocity distribution generated by the process of particle trapping. The trapped particle distribution function is obtained by means of a 1D-1V self-consistent Vlasov-Poisson simulation (with no collisions) with kinetic electrons and fixed protons. In this simulation, the initial plasma is spatially homogeneous, with Maxwellian distribution of velocities. The phase space numerical domain is discretized by 256×101 grid points in physical and velocity space, respectively.

We launch into the plasma an external driver sinusoidal electric field of the form:

$$E_D(z,t) = E_0\ g(t) \sin[k(z - v_\phi t)] \tag{3.16}$$

where $E_0 = 0.2\ \omega_p m v_{th}/e$ (m and e being the electron mass and charge, respectively), $k = 0.26\lambda_D^{-1}$, $v_\phi = 1.42 v_{th}$ and

$$g(t) = \begin{cases} \sin(\pi t/100) & t < 50 \\ 1 & 50 \leqslant t < 150 \\ \cos[\pi(t-150)/100] & 150 \leqslant t < 200 \\ 0 & t \geqslant 200 \end{cases} \tag{3.17}$$

https://doi.org/10.1017/S0022377814000877 Published online by Cambridge University Press

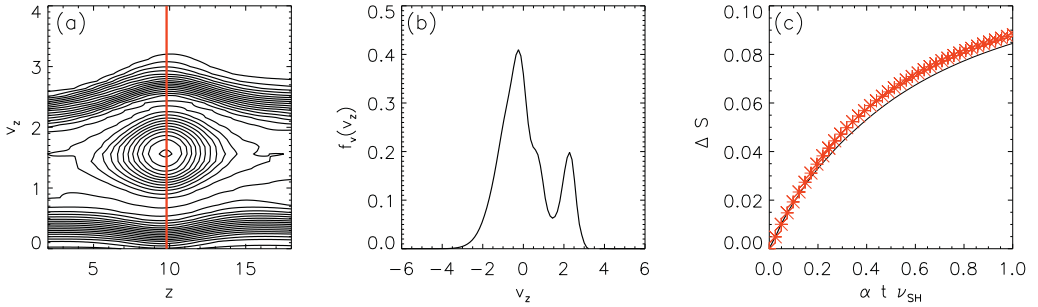


FIGURE 5. (a) Phase space portrait of the distribution function obtained through a self-consistent 1D−1V Vlasov-Poisson simulation at time $t\omega_p = 500$ zoomed in the region $x = [2, 18]$, $v = [0, 4]$. The red vertical line indicates the value of z at which we get the velocity profile $f_v(v_z)$, shown in panel (b). (c) Time evolution of the entropy growth for the Landau operator case (black solid line) and for the Dougherty operator case (red dots).

This external field is turned off once a population of trapped particles has been created. Figure 5(a) shows the phase space portrait of the electron distribution function $f_e(z, v_z)$ at a fixed instant of time, after the driver has been turned off. Here, a vortical structure, typical signature of the presence of trapped particles, is recovered. At this point, we consider the velocity profile $f_v(v_z) = f_e(z_m, v_z)$, where z_m (red vertical line in the plot) is the spatial point corresponding to the maximum velocity width of the trapping region. The velocity profile $f_v(v_z)$ is reported in Fig. 5(b).

Therefore, we build a three-dimensional velocity distribution as follows:

$$f(v_x, v_y, v_z) = C\ f_M(v_x, v_y) f_v(v_z) \tag{3.18}$$

where the constant C is chosen such that $\int f(v_x, v_y, v_z)\, d^3v = n = 1$ and

$$f_M(v_x, v_y) = \exp\left(-\frac{v_x^2 + v_y^2}{2T}\right) \tag{3.19}$$

with

$$U_z = \frac{1}{n}\int v_z f_v(v_z)\, dv_z \tag{3.20}$$

$$T = \frac{1}{n}\int (v_z - U_z)^2 f_v(v_z)\, dv_z \tag{3.21}$$

The three-dimensional velocity distribution $f(v_x, v_y, v_z)$ is used as initial condition for the direct simulations of equation (3.1), performed for both the Landau and the Dougherty operator. Figure 5(c) shows the evolution of the entropy for the case of the Landau operator (black line) and of the Dougherty operator (red dots). In this figure, as in previous examples, time has been scaled by $\alpha = 1, 3.55$ for the Landau operator and the Dougherty operator, respectively. Even in this case a slight discrepancy in the evolution of S is recovered, while a better agreement is found when the scaling factor is given the value $\alpha = 3.75$ for the Dougherty simulation.

Finally, in Figs 6(a)–(d), we directly report the velocity distribution f (evaluated at $v_x = v_y = 0$) versus v_z at four different times in the simulation. The black line in each plot represents the solution obtained when the Landau operator is considered, while the red-dashed line corresponds to the Dougherty solution. Here $\alpha = 1, 3.55$ for the Landau operator and the Dougherty operator, respectively.

https://doi.org/10.1017/S0022377814000877 Published online by Cambridge University Press

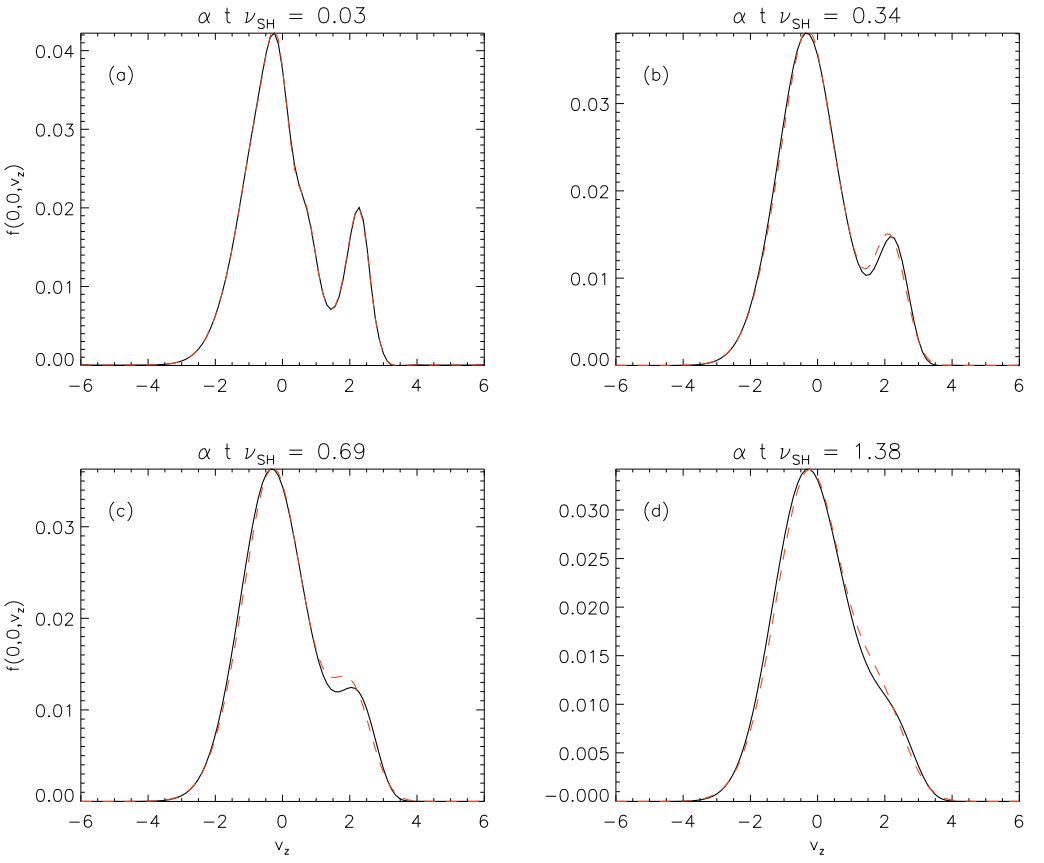


FIGURE 6. Velocity distributions obtained from the numerical solution of the Landau equation (black solid line) and of the Dougherty equation (red dashed line) at four different times $\alpha\ t_1\ \nu_{SH} = 0.03$ (a), $\alpha\ t_2\ \nu_{SH} = 0.34$ (b), $\alpha\ t_3\ \nu_{SH} = 0.69$ (c) and $\alpha\ t_4\ \nu_{SH} = 1.38$ (d).

It is worth noting that, during the relaxation process, the form of the velocity distributions display different details. In particular the Dougherty operator seems to be faster than the Landau operator, in smoothing the velocity gradients. This is consistent with the fact that, when slightly increasing more and more the value of the rescaling factor α for the Dougherty simulation, the detailed evolutions of the velocity distributions approach each other more and more. The different behavior of the two operators can be due to the different way they smooth and weight the gradients in velocity space.

4. Conclusions

In this Section we summarize the results presented above and shortly discuss possible future developments of the research on plasma collisions. We performed a detailed comparison between the Landau operator (Landau 1936) and the Dougherty operator (Dougherty 1964) by means of Eulerian kinetic simulations of a homogeneous, field-free plasma in a three-dimensional velocity space.

As a first step, by looking at the collisional relaxation processes of a bi-Maxwellian velocity distribution, we have realized that an 'ad hoc' time rescaling procedure allows

https://doi.org/10.1017/S0022377814000877 Published online by Cambridge University Press

to make the time evolution of parallel and perpendicular temperatures described by the Dougherty operator in equations (3.9), (3.10) very close to the one obtained when the full Landau integral is employed [equations (3.5), (3.6)], despite the profound mathematical differences between the two operators. Pushed by these surprising analytical findings, we employed an Eulerian algorithm to simulate numerically the return toward equilibrium of several velocity distributions (bi-Maxwellian, beam distribution, plateau distribution etc.), for which we verified that the Dougherty-Landau time rescaling factor α is the same and does not change with respect to the analytical prediction obtained for the bi-Maxwellian case.

For all velocity distributions considered in this work, the value of the factor $\alpha = 3.55$ allows to almost superpose the results for the time evolution of $T_\perp$ and $T_\parallel$ obtained in the case of the Landau operator and of the Dougherty operator. For the time evolution of the entropy, the two operators exhibit slight differences, presumably due to the different roles of the velocity gradients in the Landau and the Dougherty operator. However, we point out that the maximum relative discrepancy for the time evolution of entropy, in a one Spitzer-Harm time, is about 6%.

Our results allow to conclude that the lack of physical details that one relentlessly introduces by approximating the Landau operator with the Dougherty operator can be considered negligible compared to the advantage of having a collisional operator, the Dougherty one, that can be easily used and implemented in self-consistent Eulerian simulations and that reproduces satisfactorily the Landau collisional thermalization, once an appropriate time rescaling has been introduced.

We again emphasize that rescaling the time by the factor α in the case of the Dougherty operator, as discussed in detail previously, corresponds to rescaling the thermalization frequency ν_D in equation (3.11) by $1/\alpha$, thus slowing down the effects of the Dougherty operator.

Thanks to the time rescaling procedure described in the present paper, since the two collisional operators behave in a very similar way for about one Spitzer-Harm time, the Dougherty operator can be employed in a wide range of kinetic simulations to replace the much more complex and computationally demanding Landau operator. Indeed, it is worth noting that, for example in the case of the solar-wind plasma, the Spitzer-Harm time is significantly larger than the typical cyclotron time and plasma time (ω_p^{-1}). Therefore, the Dougherty operator can be successfully employed in place of the Landau operator to describe collisional processes in long time regime simulations of both electromagnetic and electrostatic plasmas.

To conclude this Section, we would like to point out that, since the Dougherty operator does not describe the velocity dependence of the diffusion coefficients in velocity space, we cannot assure that the time-scaling factor we determined does not change in situations where the distribution function is extremely distorted with respect to a Maxwellian one. However, the detailed comparison between Landau and Dougherty collisional operators in full self-consistent simulations will be the subject of future works.

REFERENCES

Anderson, M. W. and O'Neil, T. M. 2007a Eigenfunctions and eigenvalues of the Dougherty collision operator. *Phys. Plasmas* **14**, 052 103.

Anderson, M. W. and O'Neil, T. M. 2007b Collisional damping of plasma waves on a pure electron plasma column. *Phys. Plasmas* **14**, 112 110.

https://doi.org/10.1017/S0022377814000877 Published online by Cambridge University Press

Bhatnagar, P. L., Gross, E. P. and Krook, M. 1954 A model for collision processes in gases. I. Small amplitude processes in charged and neutral one-component systems. *Phys. Rev.* **94**, 511–525.

Dougherty, J. K. 1964 Model Fokker-Planck equation for a plasma and its solution. *Phys. Fluids* **7**, 113–133.

Dougherty, J. K. and Watson, S. R. 1967 Model Fokker-Planck equations: part 2. The equation for a multicomponent plasma. *J. Plasma Phys.* **1**, 317–326.

Driscoll, C. F., Anderegg, F., Dubin, D. H. E. and O'Neil, T. M. 2009 Trapping and frequency variability in electron acoustic waves. In: *New Developments in Nonlinear Plasma Physics (AIP Conf. Proc., 1188)*, (eds.) B. Eliasson and P. K. Shukla , pp. 272–279.

Filbet, F. and Pareschi, L. 2002 A numerical method for the accurate solution of the Fokker-Planck-Landau equation in the nonhomogeneous case. *J. Comput. Phys.* **179**, 1–26.

Hinton, F. L. and Hazeltine, R. D. 1976 Theory of plasma transport in toroidal confinement systems. *Rev. Mod. Phys.* **48**, 239–303.

Kogan, V. I. 1961 The rate of equalization of the temperatures of charged particles in a plasma. *Plasma Phys. Problem Control. Thermonuclear React.* **1**, 153.

Kumar K., D. and Das, N. 2014 Electron-ion collisional effect on Weibel instability in a Kappa distributed unmagnetized plasma. *Phys. Plasmas* **21**, 042 106.

Landau, L. D. 1936 The transport equation in the case of the Coulomb interaction. In: *Collected Papers of L. D. Landau*, Pergamon Press, pp. 163–170.

Lenard, A. and Bernstein, I. B. 1958 Plasma oscillations with diffusion in velocity space. *Phys. Rev.* **112**, 1456–1459.

Livi, S. and Marsch, E. 1986 Comparison of the Bhatnagar-Gross-Krook approximation with the exact Coulomb collision operator. *Phys. Rev. A* **34**, 533–540.

Marsch, E. 2006 Kinetic physics of the solar corona and solar wind. *Living Rev. Sol. Phys.* **3.1**, 1–100.

O'Neil, T. M. 1968 Effects of Coulomb collisions and microturbulence on plasma wave echo. *Phys. Fluids* **11**, 2420–2425.

Pareschi, L., Russo, L. G. and Toscani, G. 2000 Fast spectral methods for the Fokker-Planck-Landau Collision operator. *J. Comput. Phys.* **165**, 216–236.

Peyret, R. and Taylor, T. D. 1983 *Computational Methods for Fluid Flow*, Springer.

Pezzi, O., Valentini, F., Perrone, D. and Veltri, P. 2013a Eulerian simulations of collisional effects on electrostatic plasma waves. *Phys. Plasmas* **20**, 092 111.

Pezzi, O., Valentini, F., Perrone, D. and Veltri, P. 2013b *Phys. Plasmas* **20**, 092 111.

Pezzi, O., Valentini, F., Perrone, D. and Veltri, P. 2014a Erratum: Eulerian simulations of collisional effects on electrostatic plasma waves. *Phys. Plasmas* **21**, 019 901.

Pezzi, O., Valentini, F. and Veltri, P. 2014b Kinetic ion-acoustic solitary waves in collisional plasmas. *Eur. Phys. J.* D **68**, 128.

Spitzer, Jr, L. 1956 *Physics of Fully Ionized Gases*, Interscience Publishers.

Valentini, F., O'Neil, T. M. and Dubin, D. H. E. 2006 Excitation of nonlinear electron acoustic waves. *Phys. Plasmas* **13**, 052 303.

Vlasov, A. A. 1938 On vibration properties of electron gas. *J. Exp. Theor. Phys.* **8**, 291.

Zakharov, V. E. and Karpman, V. I. 1963 On the nonlinear theory of the damping of plasma waves. *Sov. Phys. JETP* **16**, 351–357.

https://doi.org/10.1017/S0022377814000877 Published online by Cambridge University Press